The effects of diatom pore-size on the structures and extensibilities of single mucilage molecules

Carbohydrate Research 448 (2017) 35–42

Contents lists available at ScienceDirect

Carbohydrate Research

journal homepage: www.elsevier.com/locate/carres

The effects of diatom pore-size on the structures and extensibilities of single mucilage molecules

Immanuel Sanka [a, b], Eko Agus Suyono [a, c], Parvez Alam [a, d, *]

[a] Laboratory of Paper Coating and Converting, Centre for Functional Materials, Abo Akademi University, Porthaninkatu 3, 20500 Turku, Finland
[b] Marine Study Group (KSK-Biogama), Faculty of Biology, Gadjah Mada University, Indonesia
[c] Algal Biotechnology and Engineering Unit, Biotechnology Laboratory, Faculty of Biology, Gadjah Mada University, Indonesia
[d] Institute for Materials and Processes, School of Engineering, University of Edinburgh, UK

ARTICLE INFO

Article history:
Received 26 February 2017
Received in revised form
20 April 2017
Accepted 18 May 2017
Available online 26 May 2017

Keywords:
Glucuronic acid
Mannuronic acid
Galacturonic acid
EPS
Nanopore

ABSTRACT

Diatoms secrete extracellular polymeric substances (EPS), or mucilage, around the cell wall that may serve to aid in motility and form a discrete layer that may help maintain thicker layers of EPS that have a greater role in adhesion. Mucilage molecules adhere to the diatom frustules, which are biosilica skeletons that develop from the diatom cell walls. Here, molecular dynamics methods were used to determine the characteristics of mucilage molecules as a function of pore size; notably 1,4-α-D-galacturonic acid, 1,4-β-glucuronic acid and 1,4-β-D-mannuronic acid. These uronic acids differ from each other in structure and extensibility as a function of their folding characteristics. Here, we find that when overlain upon a pore, mucilage molecules try to return to their native folded states but are restrained by their interactions with the silica surfaces. Furthermore, the extensibility of mucilage molecules over pore spaces affects the extent of mechanical energy required to straighten them. As such, different EPS molecules will affect sliding, friction and adhesion to subsequent layers of EPS in different ways. We conclude that higher EPS extensibility is homonymous with higher adhesive or frictive resistance since the molecules will be able to strain more before they reach the most extended (and thus rigid) conformation. The research herein is applicable to modern engineering as it yields insight into the biomimetic design of molecules and surfaces for improved adhesion or motility.

1. Introduction

Diatoms are mucilage-secreting unicellular microalgae with silicified cell walls (frustule). These microorganisms are often associated with biofouling problems [20] and have inherent mechanical protection from their glassy frustules. Frustules are made up of monosilicic acid, polymerised silicic acid and/or other organo-silica complexes [3]. Frustules are also ornamented with pores, the majority of which are typically between 3 and 50 nm in diameter [49], though pores below 10 nm long and 2–5 nm wide have also been reported in the literature [48]. Extracellular polymeric substances (EPS), or, mucilage, is secreted by the diatom, expressing itself through the pores, and this enables the diatoms a degree of initial motility [2] and/or initial settlement upon diverse substrates. Long-term biofouling *problematically* occurs on substrates such as pipes [22], maritime vessels [43] and membranes [38,47]. These materials often require extensive cleaning to remove biofilms formed by diatoms and other fouling micro-organisms, though in certain instances materials have to be replaced. Both cases result in unwanted economic losses. Nevertheless, there have been recent successful endeavours that utilise the combined biofouling and glass secreting characteristics of diatoms *beneficially* in advanced engineering materials [52]. Moreover, certain decorating organisms such as crabs *also benefit* from diatom biofouling by building up hierarchical architectures that they use to increase the effectiveness of carapace camouflage [42].

Mucilage molecules can be classified as either attached EPS or non-attached EPS [44]. Ford and Percival [23] reported that the predominant attached EPS carbohydrates in mucilage are β-1,3-linked glucoses with branches at Carbon-6. Mucilage consists primarily of polysaccharides, proteins, pyruvates, uronic acids, and SO_4^{2-} groups [6,23,44]. Monosaccharides of rhamnose, fucose, ribose, arabinose, xylose, mannose, galactose and glucose have

* Corresponding author. Institute for Materials and Processes, School of Engineering, University of Edinburgh, UK.
E-mail addresses: parvez.alam@ed.ac.uk, parvez.alam@abo.fi (P. Alam).

http://dx.doi.org/10.1016/j.carres.2017.05.014
0008-6215/

been identified in the diatom *A. caffeaeformis* [5], the most dominant of which are mannose, galactose and glucose [6]. Similar monosaccharidic presence has been reported by Ref. [44] as present in *Cylindrotheca closterium* and *Navicula salinarum*. In later research, Chiovitti and co-workers [14] reported the warm water extracted glucans (originating presumably from β-1-3 glucan chrysolaminaran) are predominantly intracellular. As such, it is unlikely that storage polysaccharides like β-1-3 glucan chrysolaminaran will form any large part of the initial mucilage layer, which has been described as essentially a marine gell aggregate [46]. More aged mucilage layers tend to be less sticky than fresh mucilage and contain longer molecules [50], which might in turn strengthen the mucilage layer by entanglement [46]. Though storage polysaccharides might leak to some extent through the diatom pores, they will likely be swiftly degraded by bacteria [27]. Moreover, the rate of any possible leaking will be an inverse function of the tortuosity of the path that the leaking molecules will have to take, which are in turn dependent upon the organisation of matter [1] across the diatom pore. Some of the more likely glycopolysaccharides involved in initial diatom attachment are galacturonic acid and glucuronic acid [39]. Attachment in the initial stages essentially sets up the diatom for motile gliding [36], which eventually becomes sessile attachment through the development of protuberant EPS pads, tubes and hold-fast like anchors secreted from the raphe [30,36]. Diatom gliding is also a means by which diatoms biofoul surfaces. Through gliding, the diatoms leave trails of attached secreted mucilage [28], which most likely detaches from attached underlying mucilage, or from the cell wall surface. AFM-based research by Higgins and co-workers [31] suggests that diatom settlement more commonly occurs on girdle bands, rather than on valves, which brings to light a seemingly pedantic settlement cycle in diatoms. The effectiveness of diatom settlement is most importantly a function of the surface of a material, the material characteristics and how it affects wetting [33]. In a study by Holland and co-workers [34] for example, diatoms were found to attach more strongly to PDMSe than to acid-washed glass.

Mucliage can merge with bacteria or other microorganisms to form biofilms made up predominantly of muco-polysacharrides [24], which in turn leads to biofouling-related problems such as substrate corrosion [10,21], the accumulation of contaminants such as fungi or protozoans [15], and the encouragement of macrofouling [9,16,42]. The attachment characteristics of diatom EPS are vital for successful colonisation and population growth [13]. Sessile attachment has been reported to arise from the immobile adhesion of a few diatoms, which then encourages the nucleation and ultimately adhesion of extended diatom colonies [37]. Mucilage molecules have distinct topographies and mechanical properties [29], which could suggest that EPS secretion is at some level, timed for either motility or adhesion. Adhesive mucilage has been found to be a biocomposite built into proteinous nanofibres that align in parallel [19]. A parallel arrangement such as this suggests a cellular level extrusion process takes place in the secretion of mucilage, however this concept has not as yet been documented, to the best of our knowledge.

The characteristics of attachment between diatom frustules and mucilage molecules are important in view of biofouling since they will affect the malleability or rigidity of the molecules, which will in turn affect the extensional properties of the molecules. Mucilage molecules with low extensibility and considerable rigidity are more likely to develop high stress intensities at interfaces, and may concurrently have reduced close-range contact with biofouling surfaces during the initial stages of settlement. Pore space is one feature of the frustule surface that we hypothesise affects molecular extensibility since molecules not in contact with the frustule surface are expected to try to return to their native folded states. To date, there have been no reports on the molecular mechanics of early-stage carbohydrate (EPS) secretions of diatoms and indeed, how these secretions affect motility and/or adhesion. Further, there have been no attempts to define the effects of pore space on the folding, or partial-folding characteristics of diatom EPS. In this paper, we use molecular dynamics methods to predict the effects of frustule pore sizes on the structures and extensibilities of single diatom mucilage molecules with an aim of elucidating fine balances between molecular attachment and molecular mobility.

2. Methods

Uronic acids falling under the category of *attached EPS* [44] included; 1,4-β-D-mannuronic acid, 1,4-α-D-galacturonic acid, and 1,4-β-glucoronic acid. These were constructed in Ascalaph Designer as single molecules. Each mucilage molecule was built up of 18 monomeric repeats. Silica sheets were also constructed in Ascalaph Designer in a 16 $\times$ 16 molecule array and *ab initio* simulations performed on all molecular structures to determine their partial atomic charges in preparation for molecular dynamics interaction simulations. The *ab initio* simulations, were conducted using the Firefly QC [25] package calculating electrostatic potential derived charges by MP2 (perturbation theory) alongside the 6-311+G(2d,p) basis set [18].

Molecular dynamics simulations were initially conducted on single mucilage molecules to ascertain their steady state folded structures. Following this, attachment simulations were conducted of single mucilage molecules upon two adjacent silica surfaces, separated by a distance to mimic the pore space. This separation and hence, pore size, was varied independently and in total three different nano-pore sizes were used for the simulation of four different mucilage molecules. Exact nano-pore sizes were determined using Discovery Studio Visualiser [7] as being 8.24 Å, 16.91 Å, and 30.04 Å smallest to largest, respectively. Single mucilage molecules were also simulated on complete silca sheets (with no pore space). In all porous model simulations, the entire silica sheets were given zero degrees of freedom and linear unfolded molecules positioned across the sheets with the centre of the molecule crossing over the nano-pore space and separated from the silica sheets by a distance of approximately 10 Å. For the complete sheet simulations (with no pore space) the molecules were placed lengthways across the centre of the sheet. A Monte Carlo method was used to energetically stabilise the molecule prior to molecular dynamics simulations. Molecular dynamics simulations were then conducted in vacuum using a Sheffield solvation model to perform the simulation under implicit water conditions [26]. An AMBER94 force field was used since it is focused on intermolecular and intramolecular interactions and is typically used for biomolecular modelling [12,51]. Modelling was conducted using a 5.5 fs time step and stopped at steady state. Post-simulation analyses were conducted using the Discovery Studio 4.1 Visualiser [7] to determine specific features including; angles, bends, distances, stretch, and twists.

3. Results and discussion

Mucilage molecules (EPS), more specifically; 1,4-β-D-mannuronic acid, 1,4-α-D-galacturonic acid and 1,4-β-D-glucuronic acid, were simulated under the conditions of implicit water to ascertain their folded structures at steady state. These formed α and β polysaccharides conforms. 1,4-β linkages are reported to often give rise to parallel molecular chains with intermolecular hydrogen bonding, resulting in crystalline polysaccharides [4,35,45]. In the models nevertheless, Fig. 1, β-glycosidic linkages occurring in specifically 1,4-β-D-mannuronic acid form β-type turns, which give

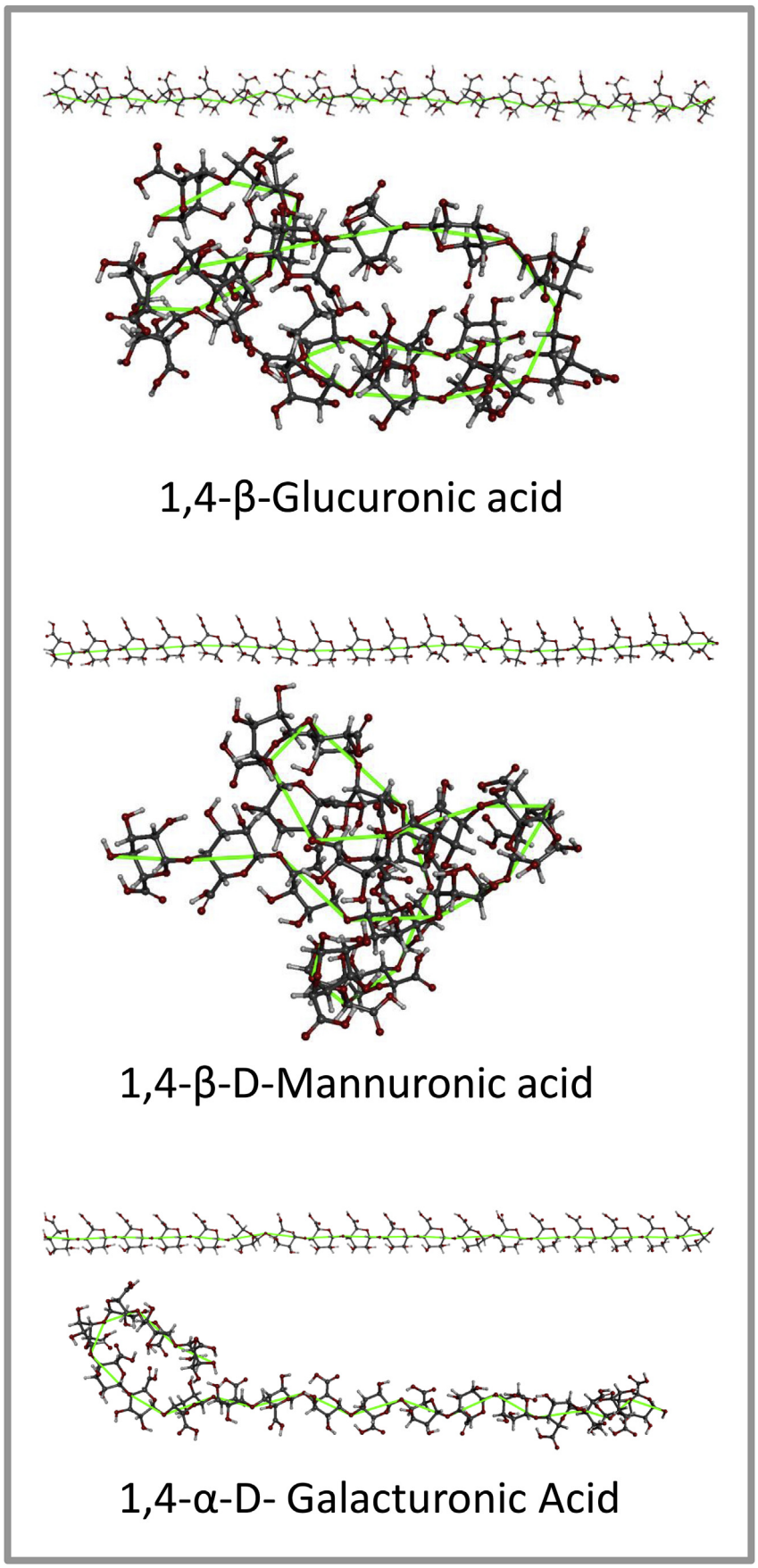

Fig. 1. Mucilage (EPS) molecules in unfolded and folded states.

rise to pleated sheet conforms in an anti-parallel-type arrangement. Contrarily, 1,4-β-glucuronic acid self-assembles into a helical arrangement, which is in turn held in place by intramolecular hydrogen bonds. 1,4-α-D-galacturonic acid is somewhat more anomalous, showing no clearly identifiable conform but rather crimping at either end while the main central bulk of the chain remains straight. The crimping also forms through hydrogen bonding however the chain is rigid due to that there structure is arranged in the α conformation, which is essentially a cross-direction molecular link giving rise to intramolecular interactions that resist conformational folding.

Figs. 2 and 3 show side and plan views, respectively, of mucilage molecule interactions across the separated and complete silica sheets. In these figures, it can be noted that 1,4-β-D-mannuronic acid and 1,4-β-D-glucuronic acid show more visible kinking, than 1,4-α-D-galacturonic acid does on the complete silica sheet. We suggest that this is related to how the silica sheet interrupts the normal folding behaviour of the individual molecules. Since 1,4-α-D-galacturonic acid folds least drammatically of the three (refer to Fig. 1, this characteristic is reflected in the way in which it kinks least radically of the three uronic acids modelled. Similarly, since both 1,4-β-D-mannuronic acid and 1,4-β-D-glucuronic acid fold most drammatically in their native states, we posit that these molecules may try to fold into their native states, but that this is obstructed somewhat by the presence of the silica sheet. These molecules might ultimately be stabilised by subsequent mucilage molecules, forming EPS networks [53]. It can furthermore be seen that for the smallest two pore sizes, the mucilage molecules form a single kink within the gap. For the highest pore size contrarily, there is no observable molecular kinking, but rather, the molecules begin to fold and twist between the silica sheets. Thus, there appears to be a critical pore size above which mucilage molecules will have greater freedom to fold towards their native states. Nevertheless, since they are also attached to the silica sheets, they are unable to complete the folding process since they are constrained at their terminal ends through secondary interactions with the silica sheets. It can also be noted that as the interaction length of molecules with the silica decrease (i.e. as the pore size increases), their ability to kink on the silica sheet is lost. As such, asymmetrically placed molecules may have greater extensibility due to kinking on silica sheets where the molecule is sufficiently long, and may lack extensibility (but gain rigidity) on the side where the molecule is too short to kink. In essence, the binding and unbinding of molecules across the substrate and gap are finding balance between the intra and intermolecular bonds that form. In this case our molecules are placed symmetrically and linearly about the pore gap and this idealisation makes it somewhat easier to assess the balance each molecule reaches at steady state. In their native states, 1,4-β-D-mannuronic acid form β-type turns; however, their orientations are rather different when attached to silica. 1,4-β-D-mannuronic acid only really develops serpentine-like β-turns when the pore space distance is smallest. The C1-C4 glycosidic link, which when taut, cannot twist easily like e.g. a C1-C3 glycosidic link and as such 1,4-β-D-mannuronic acid cannot turn easily over the pore space. At low pore sizes, 1,4-α-D-galacturonic acid being an α-configuration is able to bend, torque and twist under the influence of its secondary interactions with silica. As the pore size increases nevertheless, there are reduced interactions with silica and 1,4-α-D-galacturonic acid over the pore space returns to resisting folding as it does in its native state. In the case of 1,4-β-glucuronic acid, which in its native folded state is helically structured, twisting into its native helical structure occurs partially over the pore space and its ability to twist towards a helical arrangement increases as the pore size enlargens. Interactions with the silica cause sticking of the molecule ends and as such 1,4-β-glucuronic acid never completes its native helix structure. The structures that each molecule takes over the silica and over the pore space will affect the elasticity, or the extensibility of the polymers. The total elasticity of mucilage will be further complicated by intertwining, cross-linking, the presence of mineral-ions and molecular entanglements [11]. Figs. 2 and 3 clarify that there are significant differences for each EPS type that will affect the energies of interaction and polymeric rigidity/elasticity, and consequently, mucilage polymer adhesion or motility on substrates.

Greater molecular looseness across a diatom pore increases polymer malleability and its ability to move to achieve optimal interaction with a substrate. Excessive polymer rigidity occurs when molecular interaction energies far supersede the interatomic kinetic energies [40]. However, rigidity can also give rise to high interfacial stress intensities on deformation and as such, motility and adhesion can be seen as reliant on polymer looseness. To make a rigid molecule glide the force delivering motion from the substrate, F_m, needs only to surpass the cumulative forces of intermolecular interaction with the substrate (or an underlying substrate), $\sum F_i$, such that $F_m > \sum F_i$. If $F_m < \sum F_i$ then the molecule remains attached. Contrarily, in the case of a loose molecule that interacts with a substrate, to make the molecule motile, F_m needs to first surpass a kinematic force requirement to straighten (and rigidify) the molecule itself, F_s, after which it must surpass the additional cumulative interaction force, $\sum F_i$, such that $F_m > (F_s + \sum F_i)$. Based on this reasoning, we consider loose and malleable molecules as being more beneficial to fouling, while rigid molecules to be more beneficial to motile gliding. Moreover, here we provide insight into the means by which both adhesive (biofouling) and motile characteristics can exist simultaneously in diatoms, which are key requirements for both biofouling and gliding [54].

Closer view examples of molecular twisting and bending in 1,4-β-D-mannuronic acid on silica separated by the largest pore size are shown in Fig. 4. In this figure, a single line molecular projection of 1,4-β-D-mannuronic acid over the pore space is also provided in red. Observing this molecular projection the anfractuosity of the molecule can be seen to be > 1 and the solid molecular material is thus longer than the pore length. Over pore space therefore, 1,4-β-D-mannuronic acid has the potential for movement and has hence molecular extensibility over the pore space. This is similar to different degrees with the uronic acids, though the uronic acids fold to a lesser extent. Pores of a diatom are typically filled with mucilage molecules and as such, diatom pores are logically the regions of diatom frustules that permit superior adhesion under deformation. Consequently, diatoms that biofoul substrates should be harder to remove if they have larger and/or more pores in their frustules.Willis [49] reported that regular arrangements of well-defined pores are commonly in the range of 200–900 nm. Longer chain mucilage molecules on pores of these sizes will have greater potential in folding towards their native structures (refer to Fig. 1).

Intermolecular interaction energies for each of the polymers against the silica sheets are shown in Fig. 5 for each of the porous models. From this figure, it is evident that there is an inverse correlation between the interaction energies and the pore size in every EPS type. This is an expected correlation since as the pore size increases, the contact length of each mucilage molecule to the silica sheets decreases. Decreasing the polymer contact length has the effect of decreasing both van der Waals and hydrogen bonding [41] between proton donors and proton acceptors [32]. In the models, carbon-hydrogen bonds are noted to develop between the different mucilage molecules and the silica. This occurs when the donor is a polarised carbon atom and occurs when an acetylene group is situated adjacent to an oxygen or nitrogen atom [8]. It follows then, that, the decreasing of intermolecular energy with decreasing

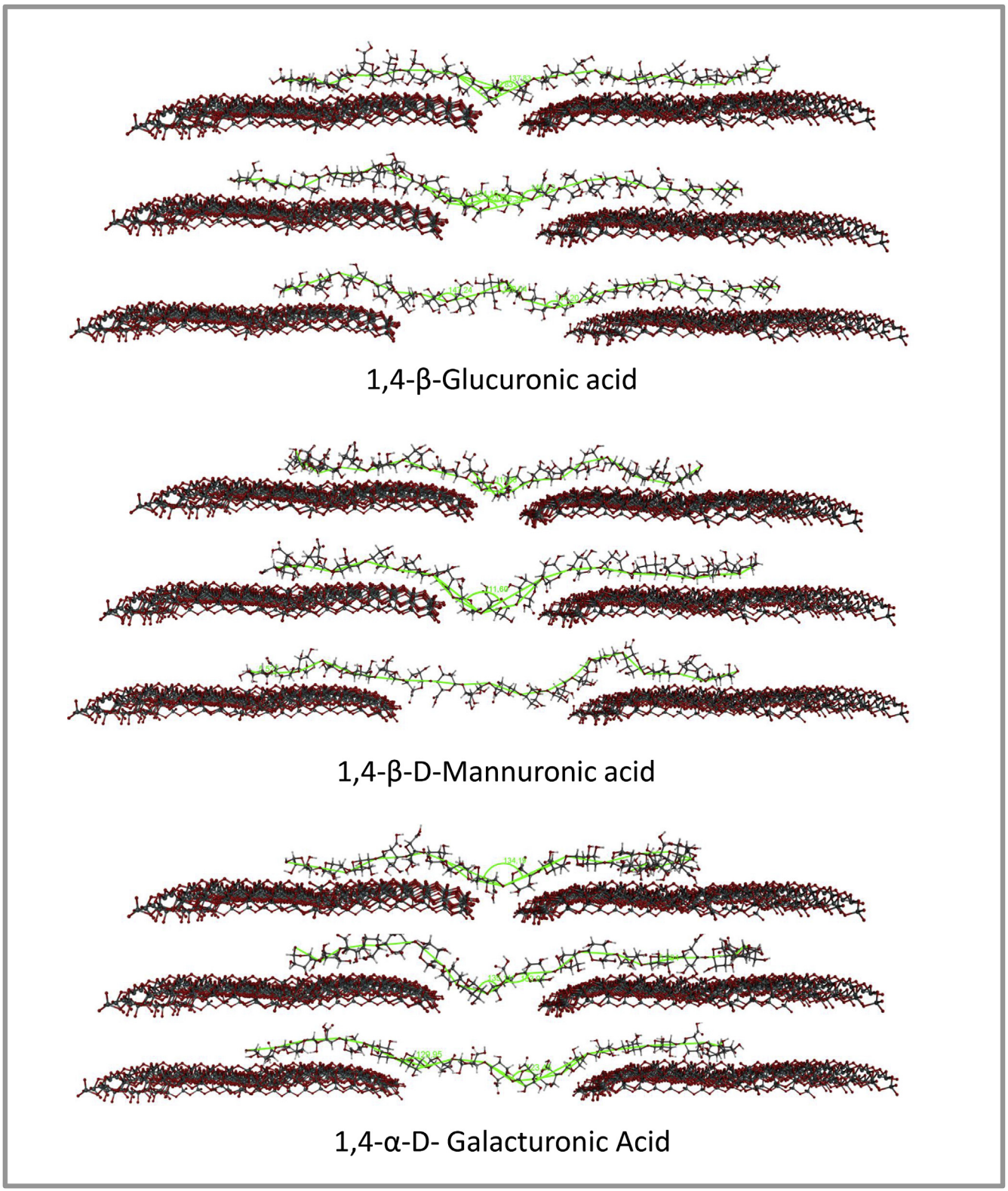

Fig. 2. Side view of EPS- porous silica sheet interactions.

molecular contact length, correlates to a loss in hydrogen bonding, which in turn will reduce the sticking power of the mucilage molecules. Moreover, as the pore size is increased, intramolecular hydrogen bonds that give rise to folding behaviours start to form in each EPS type. As a consequence, there is a tensile pull exerted upon the attached mucilage (to silica), which increases the interatomic distance for each hydrogen bond causing them to have reduced electrostatic strength.

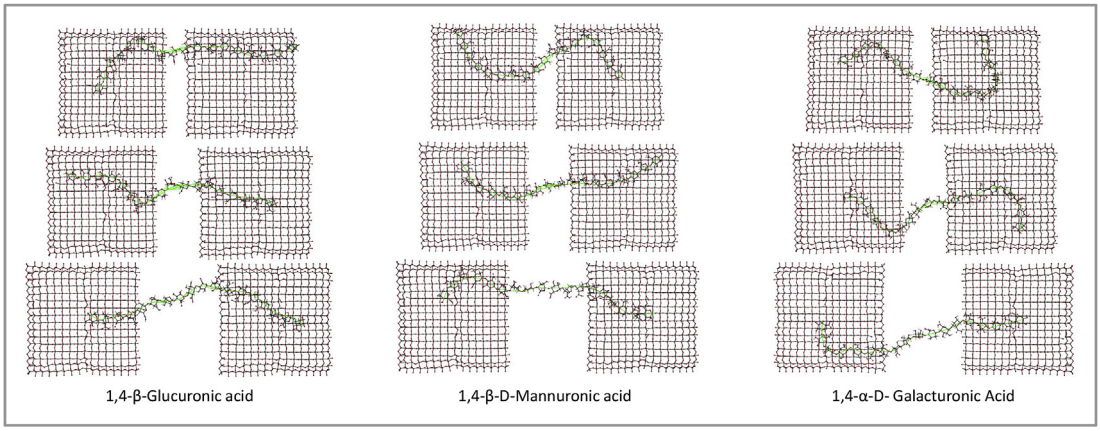

Fig. 3. EPS-porous silica sheet interactions as seen from a plan view.

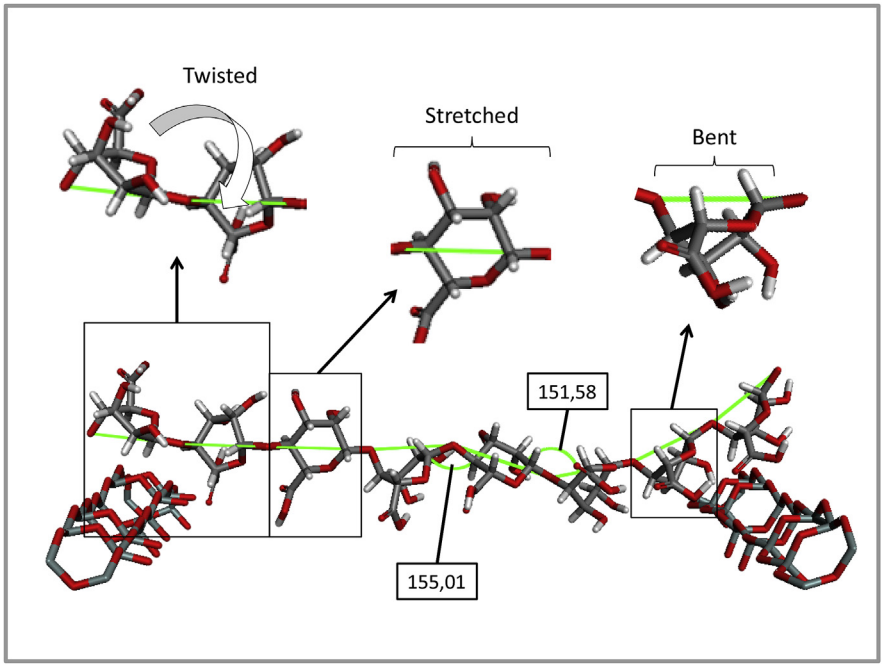

Fig. 4. Example molecular interactions over the porous silica sheet.

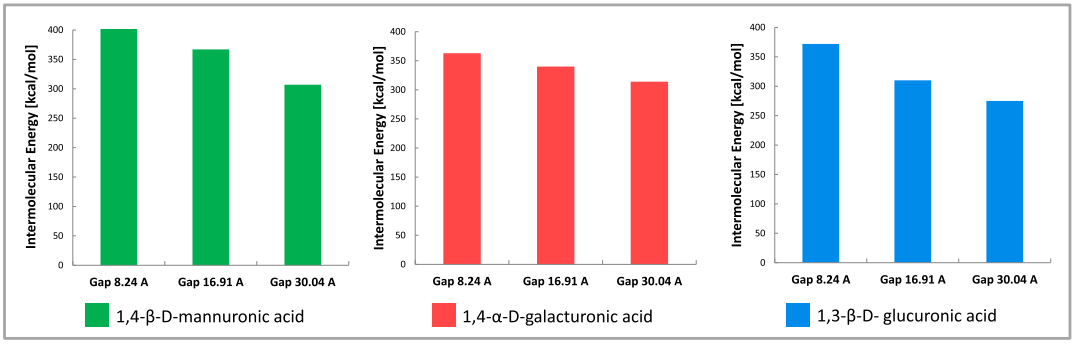

Fig. 5. Intermolecular energies of mucilage molecules as a function of increasing pore length.

4. Conclusions

We conclude that pores and pore sizes play a definitive role in altering the molecular structures and extensibilities of different mucilage molecules. This in turn can be considered analogous with the effectiveness of adhesion or motility under deformation for each EPS type, since steady state molecular structures are either rigid molecules, or loose malleable molecules. Malleable molecules with high extensibility are more likely to retain adhesion under deformation and move to energetically stable locations, whereas rigid molecules are by their nature, less able to do this so are motile. The future directions of this research include the design and development of anti-fouling surfaces and/or molecules based on how molecular-to-surface interactions guide the strength of either adhesion or slip.

Acknowledgements

We would like to thank Professor Marti Toivakka for supporting the computational facilities performed in Finland. Parvez Alam and Eko Agus Suyono would like to thank CIMO (CIMO-TM-14-9129) for financial support. Immanuel Sanka wishes to thank Dr. Bambang Retnoaji for facilitating the computational work conducted in Indonesia.

References

[1] P. Alam, T. Byholm, J. Kiivila, L. Sinervo, M. Toivakka, Calculating the permeability of model paper coating structures comprising incongruent particle shapes and sizes, Micropor. Mesopor. Mat. 117 (2009) 685–688.
[2] M. Alles, A. Rosenhahn, Microfluidic detachment assay to probe the adhesion strength of diatoms, Biofouling 31 (5) (2015) 469–480.
[3] E. Bauerlein, Biomineralization from Biology to Biotechnology and Medical Application, second ed., WILEY-VCH Verlag GmbH and Co. KGaA, Weinheim, 2004.
[4] J.M. Berg, J.L. Tymoczko, L. Stryer, Biochemistry, fifth ed., W. H. Freeman, New York, 2002. Section 11.2, Complex Carbohydrates Are Formed by Linkage of Monosaccharides. Available from: http://www.ncbi.nlm.nih.gov/books/NBK22396.
[5] N.B. Bhosle, L.V. Evans, R.G.J. Edyvean, Carbohydrate production by *Amphora coffeaeformis*, a marine biofouling diatom, Biofouling 7 (1993) 81–91.
[6] N.B. Bhosle, S.S. Sawant, A. Garg, A.B. Wagh, L.V. Evans, Chemical characterization of exopolysaccharides from the marine biofouling diatom *Amphora coffeaeformis*, Biofouling 10 (4) (1996) 301–307.
[7] Ref. Dassault Systmes BIOVIA, Discovery Studio Modeling Environment, Release 4.5, Dassault Systmes, San Diego, 2015.
[8] C. Bissantz, B. Kuhn, M. Stahl, A medicinal chemists guide to molecular interactions, J. Med. Chem. 53 (14) (2010) 5061–5084.
[9] G.D. Bixler, B. Bhusan, Biofouling: lessons from nature, Phil. Trans. R. Soc. A 370 (2012) 2381–2417.
[10] M.E. Callow, J.A. Callow, Marine biofouling: a sticky problem, Biologist 49 (1) (2002) 1–5.
[11] W.D. Callister, D.G. Rethwisch, Fundamentals of Material Science and Engineering: an Integrated Approach, John Wiley and Sons, 2012.
[12] D.A. Case, T.E. Cheatham, T. Darden, H. Gohlke, R. Luo, K.M. Merz, A. Onufriev, C. Simmerling, B. Wang, R.J. Woods, The amber biomolecular simulation programs, J. Comput. Chem. 26 (16) (2005) 1668.
[13] A. Chiovitti, M.J. Higgins, R.E. Harper, R. Wetherbee, A. Bacic, The complex polysaccharides of the raphid diatom *Pinnularia viridis* (Bacillariophyceae), J. Phycol. 39 (2003) 543–554.
[14] A. Chiovitti, P. Molino, S.A. Crawford, R. Teng, T. Spurck, R. Wetherbee, The glucans extracted with warm water from diatoms are mainly derived from intracellular chrysolaminaran and not extracellular polysaccharides, Eur. J. Phycol. 39 (2007) 117–128.
[15] A. Davies, P. Williamson, Marine Biofouling: a sticky problem, NERC News (35) (April 1995) 25–27 (Marine BioFoulNet).
[16] L. Delauney, C. Compere, Lehaitre, Biofouling protection for marine environmental sensors, Ocean. Sci. (6) (2010) 503–511.
[18] J. Deng, A.T.B. Gilbert, P.M.W. Gill, Communication: efficient counterpoise corrections by a pertubative approach, J. Chem. Phys. 135 (2011) 081105.
[19] T.M. Dugdale, R. Dagastine, A. Chiovitti, R. Wetherbee, Diatom adhesive mucilage contains distinct supramolecular assemblies of a single moduluar protein, Biophys. J. 90 (2006) 2987–2993.
[20] L.V. Evans, Marine biofouling, in: C.A. Lembi, J.R. Waaland (Eds.), Algae and Human Affairs, Cambridge Univ. Press, Cambridge, 1988.
[21] H.C. Flemming, Biofouling in water treatment, Biofouling Biocorrosion Industrial Water Syst. (1991) 47–80.
[22] H.C. Flemming, Biofouling in water systems cases, causes and countermeasures, Appl. Microbiol. Biotechnol. 59 (2002) 629–640.
[23] C.W. Ford, E. Percival, The carbohydrates of Phaeodactylum tricornutum. Part I. Preliminary examination of the organism, and characterization of low molecular weight material and of a glucan, J. Chem. Soc. (1965) 7035–7041.
[24] T. Gehrke, W. Sand, Interactions between microorganisms and physicochemical factors cause MIC of steel pilings in harbours (ALWC), NACE Int. Corros. (2003) 1–8.
[25] A.A. Granovsky, Firefly Version 8, 2015. http://classic.chem.msu.su/gran/firefly/index.html.
[26] J.A. Grant, B.T. Pickup, M.J. Sykes, C.A. Kitchen, A. Nicholls, A simple formula for dielectric polarization energies: the Sheffield Solvation Model, Chem. Phys. Lett. 441 (2007) 163–166.
[27] K. Haynes, T.A. Hoffman, C.J. Smith, A.S. Ball, G.J.C. Underwood, A.M. Odborn, Diatom-derived carbohydrates as factors affecting bacterial community composition in estuarine sediments, Appl. Environ. Microbiol. 73 (19) (2007) 6112–6124.
[28] M.J. Higgins, S.A. Crawford, P. Mulvaney, R. Wetherbee, The topography of soft, adhesive diatom trails as observed by atomic force microscopy, Biofouling 16 (2–4) (2000) 133–139.
[29] M.J. Higgins, S.A. Crawford, P. Mulvaney, R. Wetherbee, Characterization of the adhesive mucilages secreted by live diatom cells using atomic force microscopy, Protist 153 (2002) 25–38.
[30] M.J. Higgins, P. Mulvaney, R. Wetherbee, The structure and nanomechanical properties of the adhesive mucilage that mediates diatom-substratum adhesion and motility, J. Phycol. 39 (2003) 1181–1193.
[31] M.J. Higgins, J.E. Sader, P. Mulvaney, R. Wetherbee, Probing the surface of living diatoms with atomic formce microscopy: the nanostructure and nanomechanical properties of the mucilage layer, J. Phycol. (2003b) 722–732.
[32] A. Hinchliffe, Molecular Modelling for Beginners, John Wiley and Sons, 2003.
[33] O.M. Hodson, J.P. Monty, P.J. Molino, R. Wetherbee, Novel whole cell adhesion assay of three isolates of the fouling diatom *Amphora coffeaeformis* reveal diverse responses to surface of different wettability, Biofouling 28 (4) (2012) 381–393.
[34] R. Holland, T.M. Dugdale, R. Wetherbee, A.B. Brennan, J.A. Finlay, J.A. Callow, M.E. Callow, Adhesion and motility of fouling diatoms on a silicone elastomer, Biofouling 20 (6) (2004) 323–329.
[35] H. Lodish, A. Berk, S.L. Zipursky, P. Matsudaira, D. Baltimore, J. Darnell, Molecular Cell Biology, fourth ed., W. H. Freeman, New York, 2000. Section 2.1, Covalent Bonds. Available from: http://www.ncbi.nlm.nih.gov/books/NBK21595.
[36] P.J. Molino, R. Wetherbee, The biology of biofouling diatoms and their role in the development of microbial slimes, Biofouling 24 (5) (2008) 365–379.
[37] P.J. Molino, E. Campbell, R. Wetherbee, Development of the initial diatom microfouling layer on antifouling and fouling-release surfaces in temperate and tropical Australia, Biofouling 25 (8) (2009) 685–694.
[38] L.D. Nghiem, S. Hawkes, Effects of membrane fouling on the nanofiltration of pharmaceutically active compounds (PhACs): mechanisms and role of membrane pore size, Sep. Purif. Technol. 57 (2007) 176–184.
[39] N. Poulsen, N. Kroger, M.J. Harrington, E. Brunner, S. Paasch, M.T. buhmann, Isolation and biochemical characterization of underwater adhesives from diatoms, Biofouling 30 (4) (2014) 513–523.
[40] D. Reger, S. Goode, D. Ball, Chemistry: Principle and Practice, Cengage Learning, 2009.
[41] D.S. Rimai, D.J. Quesnel, The adhesion of spherical particles: contributions of Van Der Waals and electrostatic interactions, J. Adhesion 78 (5) (2002) 413–429.
[42] I. Sanka, E.A. Suyono, A. Rivero-Muller, P. Alam, Carapace surface architectures facilitate camouflage of the decorator crab *Tiarinia cornigera*, Acta Biomater. 41 (2016) 52–59.
[43] M.P. Schultz, Effects of coating roughness and biofouling on ship resistance and powering, Biofouling 23 (2007) 331–341.
[44] N. Staats, B. de Winder, L.J. Stal, L.R. Mur, Isolation and characterization of extracellular polysaccharides from the epipelic diatoms *Cylindrotheca closterium* and *Navicula salinarum*, Eur. J. Phycol. 34 (2) (1999) 161–169.
[45] I.W. Sutherland, Microbial Extracellular Polymeric Substances: Characterization, Structure and Function, Springer Science and Business Media, 2012.
[46] V. Svetlicic, V. Zutic, G. Pletikapic, T.M. Radic, Marine polysaccharide networks and diatoms at the nanometric scale, Int. J. Mol. Sci. 14 (2013) 20064–20078.
[47] D. Vogel, A. Simon, A.A. Alturki, B. Bilitewski, W.E. Price, L.D. Nghiem, Effects of fouling and scaling on the retention of trace organic contaminants by a nanofiltration membrane: the role of cake-enhanced concentration polarisation, Sep. Purif. Technol. 73 (2010) 256–263.
[48] E.G. Vrieling, W.W.C. Gieskes, T.P.M. Beelen, R.A. Van Santen, Diatom silica biomineralization: at nanoscale level a chemically uniform process, J. Phycol. 36 (2000) 70.
[49] L. Willis, K.M. Page, D.S. Broomhead, E.J. Cox, Discrete free-boundary reaction-diffusion model of diatom pore occlusions, Plant Ecol. Evol. 143 (3) (2010) 297–306.
[50] A. Willis, A. Chiovitti, T.M. Dugdale, R. Wetherbee, Characterization of the extracellular matrixof Phaeodactylum tricornutum (Bacillariophyceae): structure, composition and adhesive characteristics, J. Phycol. 49 (5) (2013) 937–949.
[51] L. Yang, C.H. Tan, M.J. Hsieh, J. Wang, Y. Duan, P. Cieplak, J. Caldwell,

P.A. Kollman, R. Luo, New-generation amber united-atom force field, J. Phys. Chem. B (110) (2006) 13166–13176.
[52] M. Zusron, I. Sanka, M. Nuhamunada, Y. Damayanti, S. Nopitasari, A.B. Kusuma, E.F.C. Ningrum, A.R. Rahmawati, N. Zakiyah, D.A. Islami, C.B. Prabaswara, M. Adhikari, E.A. Suyono, P. Alam, Glass coating natural fibres by diatomisation: a bright future for biofouling technology, Mater Today Commun. (7) (2016) 81–88.
[53] V. Svetlicic, V. Zutic, G. Pletikapic, T.M. Radic, Marine polysaccharide networks and diatoms at the nanometric scale, Int. J. Mol. Sci. (14) (2016) 20064–20078.
[54] M.R.M. Kapinga, R. Gordon, Cell attachment in the motile colonial diatom bacillaria paxillifer, Diatom Res. 7 (1992) 215–220.